

STATISTICAL MODELING OF THERMAL-RADIATION TRANSFER IN NATURAL-CONVECTION TURBULENT DIFFUSION FLAMES. 2. FLAME ABOVE A GAS BURNER

A. Yu. Snegirev

UDC 536.46:614.841.41

Natural-convection turbulent diffusion propane flames in air have been modeled numerically. The statistical method (Monte Carlo method) has been used for calculation of thermal-radiation transfer. In modeling the emission of radiation, we allowed for turbulent fluctuations of temperature. The data obtained have been compared to the results of measurements of the concentrations of the main components (fuel, oxygen, and carbon dioxide and monoxide), mean temperature and velocity and their turbulent fluctuations, the profiles of the emitted heat fluxes, and the total amount of emitted energy.

Introduction. Natural-convection turbulent diffusion flames are of special interest in studying fires. Their shape, structure, and dynamics are determined by the effect of the buoyancy force and are independent of the momentum of a fuel jet. The numerical value of the corresponding criterion (Froude number $Fr = V_{\text{fuel}}/\sqrt{gD}$) is much less than unity (10^{-3} – 10^{-2}). A large amplitude of turbulent fluctuations of all parameters is typical of these flames; therefore, they are difficult to model in detail [1]. Of great difficulty is calculation of radiation heat fluxes emitted by the flame and incident on remote surfaces. However, this information is of fundamental importance for determination of the rate of warming-up, the gasification and thermal degradation of fuel material, the delay time of ignition, and the velocity of propagation of the flame.

In the previous numerical investigations of natural-convection turbulent diffusion flames, thermal-radiation transfer was modeled at different degrees of detail. In the simplest case, e.g., [2, 3], the thermal effect of reaction was corrected by a value corresponding to radiation heat loss. In the case of small dimensions of the flame, it was assumed that the flame is optically thin and the emitted energy is not absorbed [1]. It is obvious that these approaches do not provide data on the heat fluxes emitted by the flame. For calculation of these fluxes, the flow method was used in [4, 5] and the discrete-transfer method in [6, 7]. The limitations of these and other existing approaches and also the description of the statistical method (Monte Carlo method), where these limitations have been overcome to a great extent, are given in [8].

In the present work, the statistical method, in combination with the models of turbulence and combustion [8], is used for calculation of the emission, transfer, and absorption of thermal radiation in natural-convection turbulent diffusion flames above a gas burner with a specified flow rate of the fuel. Results of statistical modeling of radiation transfer are compared to calculation by the flow method and experimental data. To test the model we used the fields of the mean velocity, temperature, and concentrations of the components, the radiation heat fluxes, and the fluctuation characteristics of velocity and temperature measured in [9, 10]. It is shown that, in contrast to the flow method, the statistical approach gives satisfactory agreement with experiment and the consumption of processing time by its implementation does not exceed the consumption by solution of other problems (calculation of the velocity and pressure fields, solution of scalar equations of transfer).

Problem Formulation. We have conducted numerical modeling of the combustion of propane in air above a round burner of diameter 0.3 m. Experimental study of the process has been made in [9, 10], where the flow rate of propane provided a thermal power of the flame of 15.8 to 37.9 kW. The equations of the model have been given in [8].

The calculations showed that the boundary conditions imposed on the characteristics of turbulence in the outlet cross section of the burner greatly affect the shape of the flame. This is caused by the fact that the k - ϵ turbulence

model does not give a qualitative description of flow in the region adjacent to the surface of fuel outflow, where it is not quite turbulent [2, 3, 8]. By virtue of this, the numerical values of k_{fuel} and $\varepsilon_{\text{fuel}}$ are the parameters of the model and must be specified so as to ensure the best agreement between calculations and experiments. To determine these parameters, in what follows we used the characteristic scales of length and velocity

$$L_B = \left(\frac{\dot{Q}}{C_{P0} \rho_0 T_0 \sqrt{g}} \right)^{2/5}, \quad V_B = \sqrt{g L_B},$$

which are formed for reasons of dimensionality with account for the dominant role of the buoyancy force [11].

Turbulent parameters in the fuel flow in the outlet cross section of the burner were calculated as

$$k_{\text{fuel}} = \alpha_k V_B^2, \quad L_{t,\text{fuel}} = \alpha_L L_B, \quad \varepsilon_{\text{fuel}} = \frac{k_{\text{fuel}}^{3/2}}{L_{t,\text{fuel}}}.$$

The following values of the turbulent viscosity and the time scale correspond to these parameters:

$$\mu_{t,\text{fuel}} = \alpha_k^{1/2} \alpha_L C_\mu \rho V_B L_B, \quad \tau_{t,\text{fuel}} = \alpha_k^{-1/2} \alpha_L L_B / V_B,$$

where $C_\mu = 0.09$. The results of the calculations are most sensitive to a numerical value of α_L . For small α_L (i.e., at low numerical values of $\mu_{t,\text{fuel}}$ and $\tau_{t,\text{fuel}}$) there form elongated flames with a very narrow zone where the fuel and the oxidizer are mixed and the reaction occurs. In the opposite limit (at large α_L), a shorter flame with a wider zone of mixing and reaction is obtained. As is shown below, at $\alpha_k = 0.1$ and $\alpha_L = 0.3$ the length of the flame and the distribution of the concentrations in it are in satisfactory agreement with experimental data [9].

In formulating the boundary conditions for the parameters of turbulence, the tangential velocity, and the enthalpy on solid surfaces, we used the standard method of near-wall functions. The surface temperatures were taken constant and equal to the initial temperature. On open boundaries, the dynamic pressure was assumed to be zero. On the inlet portions of the open boundaries, initial values were assigned to all the transferred parameters. Where the flow leaves the computational region, the derivatives of all the parameters were assumed to be zero. The emissivities of the wall surfaces were taken to be 0.7, while the emissivity of the outlet cross section of the burner was taken to be 1.0. When the statistical method was used, it was assumed that photons reaching the open boundaries escape from the computational region. At the initial instant of time, it was taken that air is motionless and has a temperature of 298 K and a pressure of 1 atm and that the mass fractions of nitrogen and oxygen are 0.77 and 0.23 respectively. The initial values of the turbulence parameters are $k_0 = 10^{-3} \text{ m}^2/\text{sec}^2$ and $\varepsilon_0 = 10^{-3} \text{ m}^2/\text{sec}^3$.

Numerical Method. The transfer equations given in [8] were solved numerically by the control-volume method [12] in the region with horizontal dimensions $1.2 \times 1.2 \text{ m}$ and height 1.5 m . The surface of the burner which was at the center of the region coincided with the floor level. A nonuniform computational grid had 102,400 meshes ($40 \times 40 \times 64$). The bunching of the grid in the flame zone allowed better resolution of large gradients in this zone. There were 264 grid meshes on the fuel surface and about 40 grid meshes over the flame height. The smallest space step was 0.015 m along the vertical and 0.01875 along the horizontal, which provided a weak dependence of the solution on the grid mesh.

The space derivatives in the diffusion terms were approximated by central differences; a TVD upwind scheme with a Van Albada limiter was used for convective terms [12]. The time derivatives were approximated by the implicit method of first order of accuracy. The scalar quantities and projections of velocity were determined on biased grids. The continuity equation within small Mach numbers was fulfilled using the procedure of pressure correction. The dynamic pressure was found from the Poisson equation, which was solved by the multigrid method with the use of a V-cycle between nested grids of four levels. The method of successive upper relaxation over lines was used as a smoothing algorithm in the multigrid method and for solving differential equations of transfer. The criterion of convergence of iterations on each time step was taken to be fulfilled when the residual of the differential equations, which was normalized to the characteristic flow through the mesh edges, decreased below 10^{-4} in all the control volumes. In calculating the parameters on a new time layer, all the transfer equations and the procedure of pressure correction were

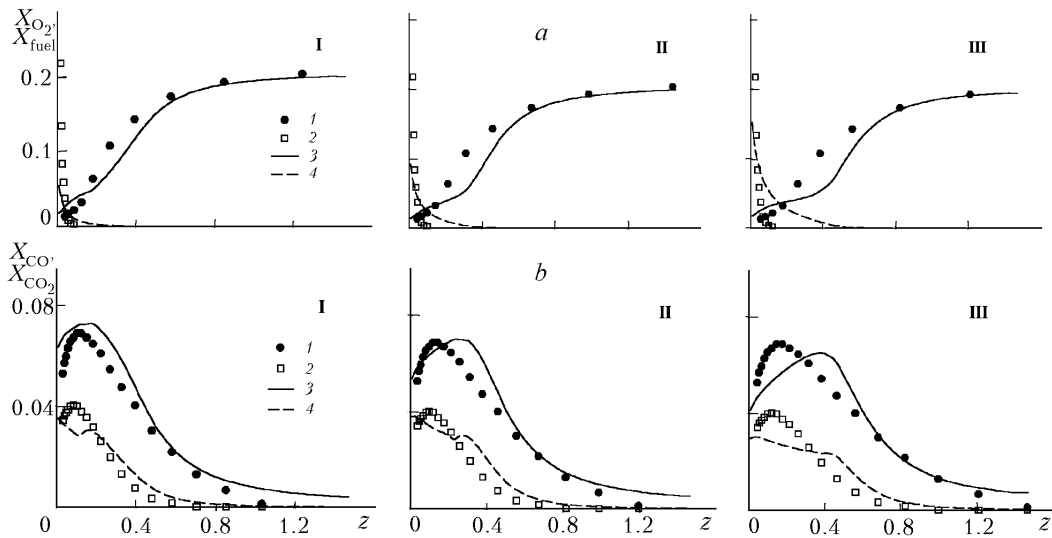


Fig. 2. Mole fraction of the components on the flame axis: (a) 1) oxygen [9]; 2) propane [9]; 3) oxygen [the present model]; 4) propane [the present model]; (b) 1) carbon dioxide [9]; 2) carbon monoxide [9]; 3) carbon dioxide [the present model]; 4) carbon monoxide [the present model]. I, $\dot{Q} = 15.8$; II, 22.9, and III, 37.9 kW. z , m.

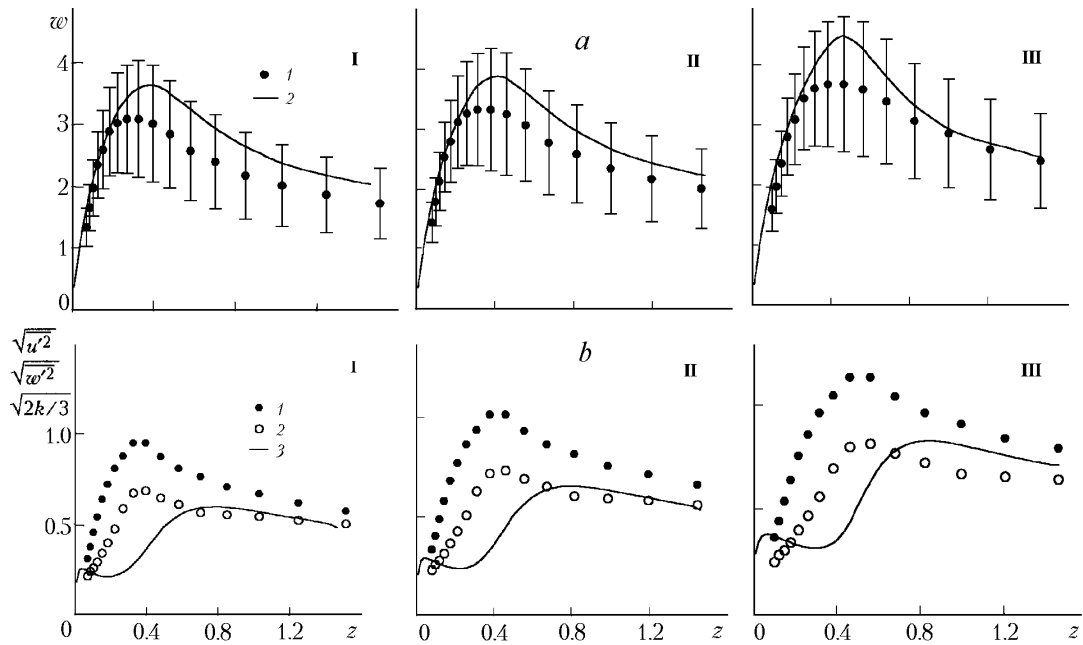


Fig. 3. Mean velocity on the flame axis (a) [1] experiment [9] (segments show the root-mean-square fluctuation of the vertical velocity); 2) the present model and its fluctuation characteristics (b) [1] $\sqrt{u'^2}$ [9]; 2) $\sqrt{u'^2}$ [9]; 3) $\sqrt{2k/3}$ [the present model]). I, II, and III, see Fig. 2 for the notation. ω , m/sec; z , m.

nonisotropic in the flame zone, which goes beyond the scope of the assumptions made in derivation of the k - ϵ model. At the same time, satisfactory agreement between the calculated and measured values is observed in the upper part of the torch, where fluctuations are more isotropic.

Figure 4, where the calculated and experimental profiles of temperature and its root-mean-square fluctuation on the flame axis are compared, indicate their close agreement within the studied range of flow rates of the fuel.

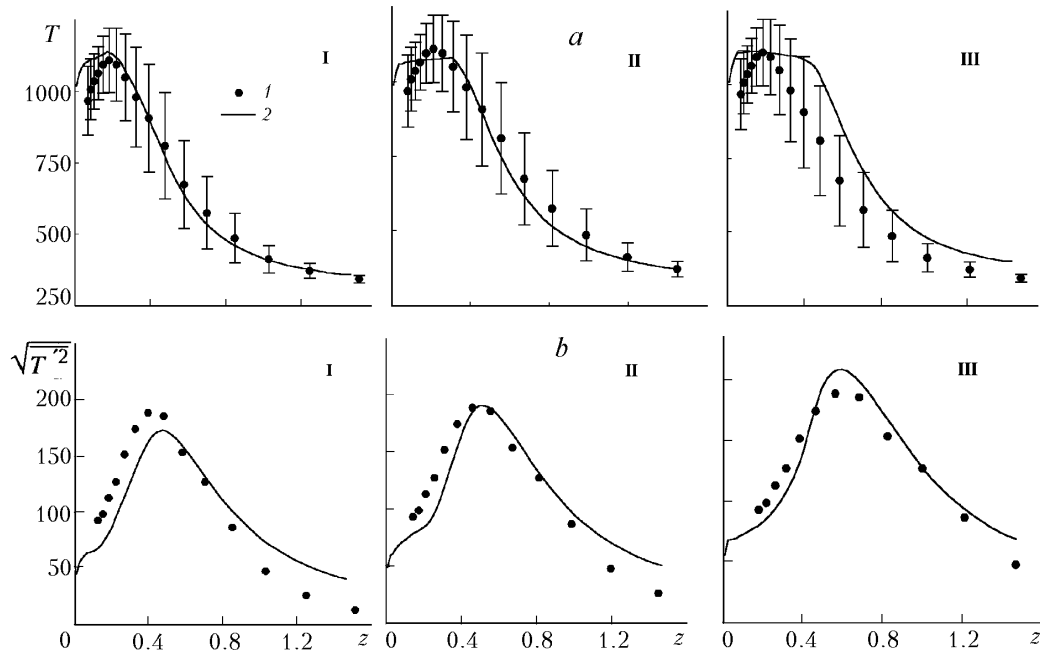


Fig. 4. Mean temperature T on the flame axis (a) and its root-mean-square fluctuation $\sqrt{T'^2}$ (b) [1) experiment [9]; 2) the present model]. I, II, and III, see Fig. 2 for the notation. T , K; z , m.

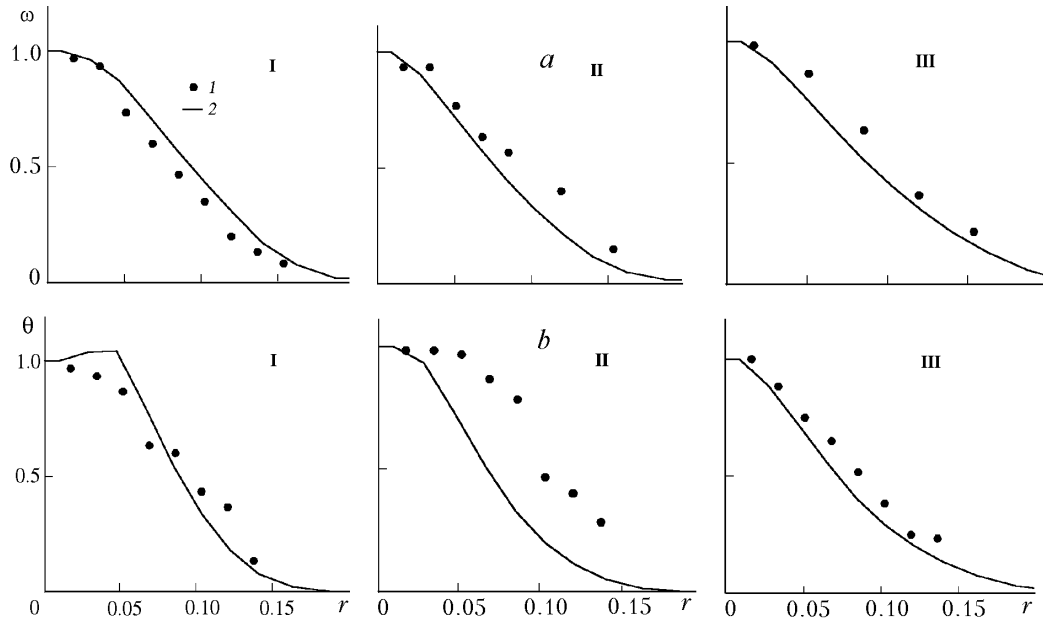


Fig. 5. Dimensionless radial profiles of vertical velocity (a) and temperature (b) [1) experiment [9]; 2) the present model]. I) $z = 0.2$; II) 0.4 , III) 0.6 m; $\dot{Q} = 37.9$ kW. r , m.

The radial profiles of the dimensionless vertical velocity $\omega = w(r, z)/(0, z)$ and the temperature $\theta = (T(r, z) - T_0)/(T(0, z) - T_0)$ at different heights z above the burner are shown in Fig. 5. It should be noted that the width of the calculated temperature profile in the flame zone (at a height of 0.4 m) is appreciably smaller than the measured one, which, as above, indicates the limitedness of the turbulence model used.

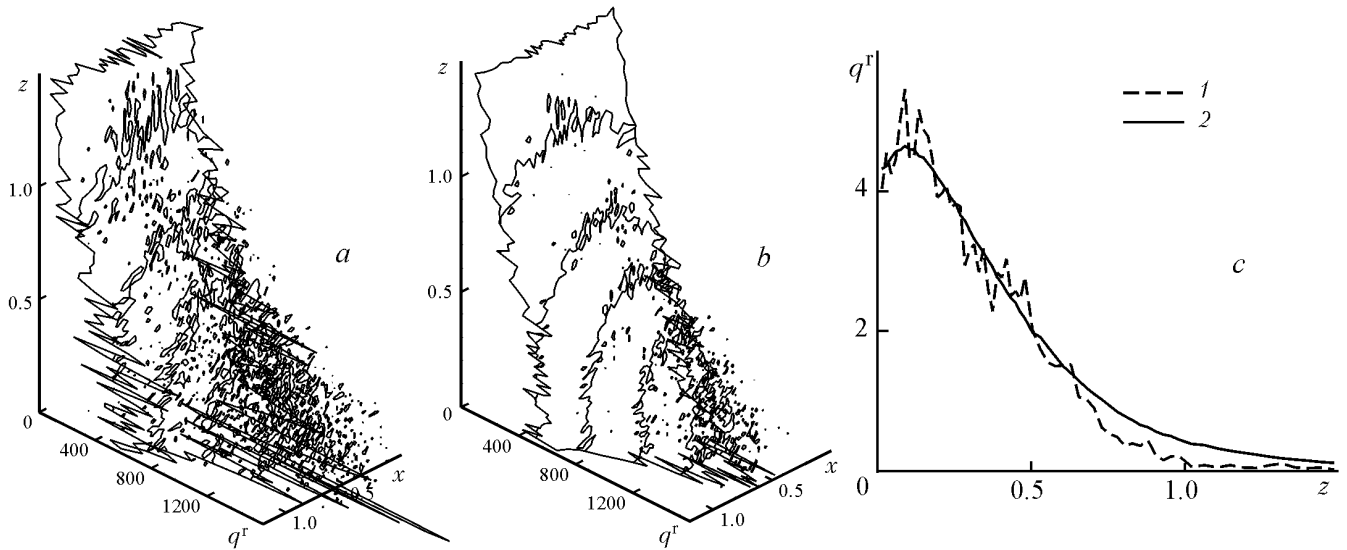


Fig. 6. Statistical fluctuations of the radiation heat flux incident on a plane surface at a distance of 0.6 m from the flame axis (a and b) [total number of photons: a) 10^5 ; b) 10^6] and flow (averaged over the polar angle) incident on a cylindrical surface of radius 0.3 m (c) [total number of photons: 1) 10^4 ; 2) $4 \cdot 10^6$]. $\dot{Q} = 22.9 \text{ kW}$. $z, x, \text{ m}$; $q, \text{ W/m}^2$.

By and large, the given analysis allows one to draw the conclusion that this model reproduces the results of measurement of the concentration, temperature, and velocity and of their fluctuations rather adequately.

Thermal-radiation transfer. The radiation heat flux calculated by the Monte Carlo method is susceptible to statistical fluctuations, which can be rather high with an insufficient number of photons emitted by internal control volumes and boundary surfaces. To evaluate the effect of the number of photons on the calculation results we changed their total number $N_{\text{vol max}} + N_{\text{surf max}}$ from 10^4 to $4 \cdot 10^6$. Radiation heat fluxes incident on a vertical plane, obtained at different numbers of photons, are shown in Fig. 6a and b.

The space distribution of the incident radiation heat flux becomes smooth only at a rather large number of emitted photons. It should be noted that in engineering applications calculations are aimed at obtaining not only the instantaneous value of the heat flux (in nonstationary processes) but also the surface temperature, which depends on the dose of the heat flux received by the surface during a long time interval. If the indicated interval involves many time steps and the procedure of photon emission is repeated at each step, the resultant dose displays only slight statistical fluctuations of the solution due to the time-averaging of the flow. In other words, the integrated dose of thermal radiation (and the temperature of the receiving surface) is much less sensitive to the total number of emitted photons at each time step than the instantaneous radiation flux.

Figure 6c shows the calculated vertical profile of the radiation heat flux incident on a cylindrical thermal surface of radius 0.3 m (the flux is obtained by averaging over a polar angle). We note that even at a very small number of emitted photons of this flux the amplitude of statistical fluctuations is considerably smaller than the expected errors of the turbulence and combustion models and than the experimental error.

Since the flow method is the simplest and most widespread in engineering practice (see, e.g., [13]), it is of interest to compare results of statistical modeling and of calculation by this method. In the case of employment of this method, the source term in the equation of enthalpy transfer (divergence of the radiation heat flux) was calculated as

$$\frac{\partial q_j^r}{\partial x_j} = -4K_{\text{abs}}(\sigma T^4 - E),$$

where the density of radiation energy $E = (E_x + E_y + E_z)/3$ was determined by solving one-dimensional equations for each component E_x , E_y , and E_z (see [8] for details). A comparison of the divergence of the radiation heat flux

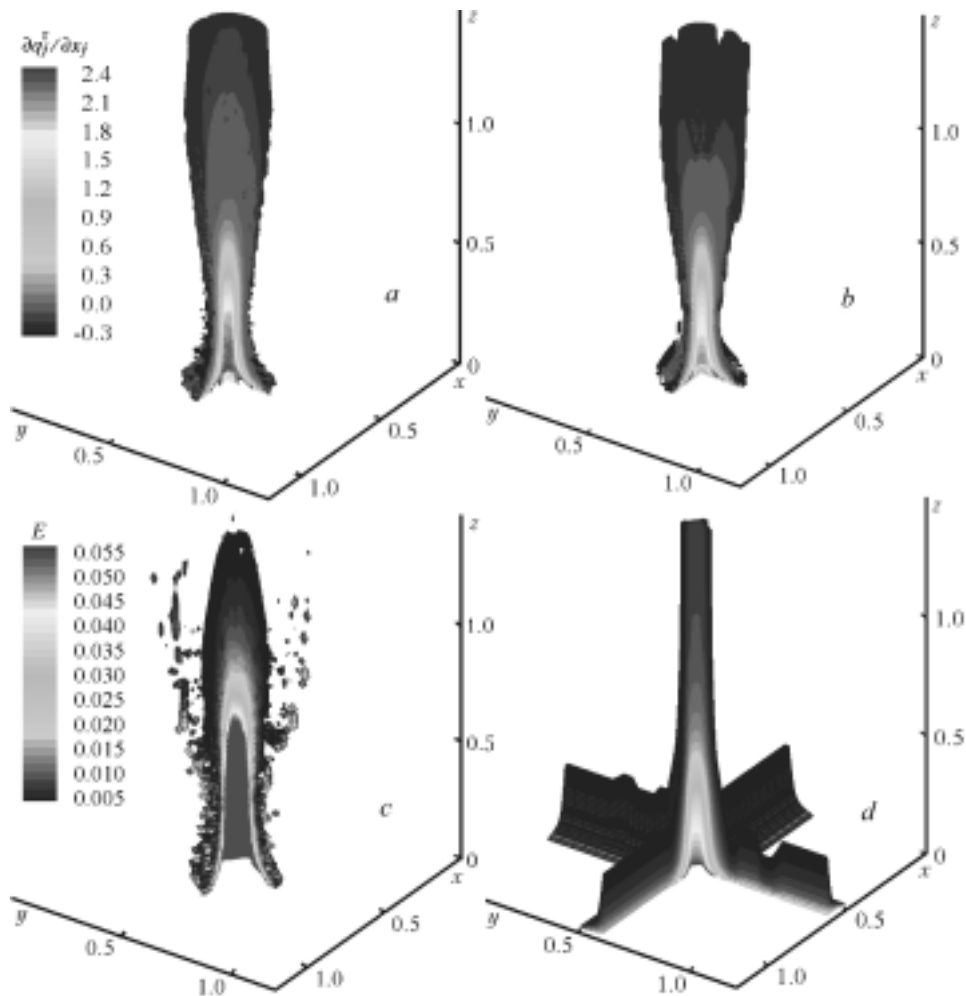


Fig. 7. Divergence of the radiation heat flux $\partial q_j^r/\partial x_j$ (a and b) and the density of radiation energy E (c and d) calculated by the statistical (a and c) and flow (b and d) methods. $\partial q_j^r/\partial x_j$, MW/m³; E , MW/m²; x , y , z , m.

$\partial q_j^r/\partial x_j$, the density of radiation energy E , and the space distribution of the radiation fluxes on a vertical surface is given in Figs. 7 and 8.

Calculation shows that the flow method reproduces the total balance of radiation energy adequately and does not lead to a substantial distortion of the field $\partial q_j^r/\partial x_j$ (Fig. 7a and b). Owing to this the method can be used as an approximate approach in modeling heat transfer inside the flame zone.

However, for the heat fluxes incident on surfaces which are at a distance from the flame the methods under discussion give strongly varying results. We note that the flow method is derived on the assumption that the radiation intensity inside the six segments of the solid angle is constant (the axes of each segment are parallel to the coordinate axes [13]). This assumption means that the radiation energy propagates only along the coordinate axes and is not redistributed in other directions. As a result, the field of the density of radiation energy E (radiation energy in volume unit multiplied by the velocity of light) which is calculated by the flow method (Fig. 7d) qualitatively differs from the field calculated by the statistical method (Fig. 7c). Concentration of the radiation energy in six directions leads to the focusing of the calculated radiation fluxes incident on the surfaces surrounding the source. A comparison of the incident heat fluxes is presented in Fig. 8. Despite the fact that the total amount of energy emitted by the flame remains the same, the space distribution of the radiation flux turns out to be significantly different. The flow method gives a geometric projection of the flame shape onto the receiving surface, which is perpendicular to the coordinate axis (Fig. 8a). This means that the method can lead to a great error in calculation of the radiation fluxes (and doses) from localized sources which are incident on remote surfaces.

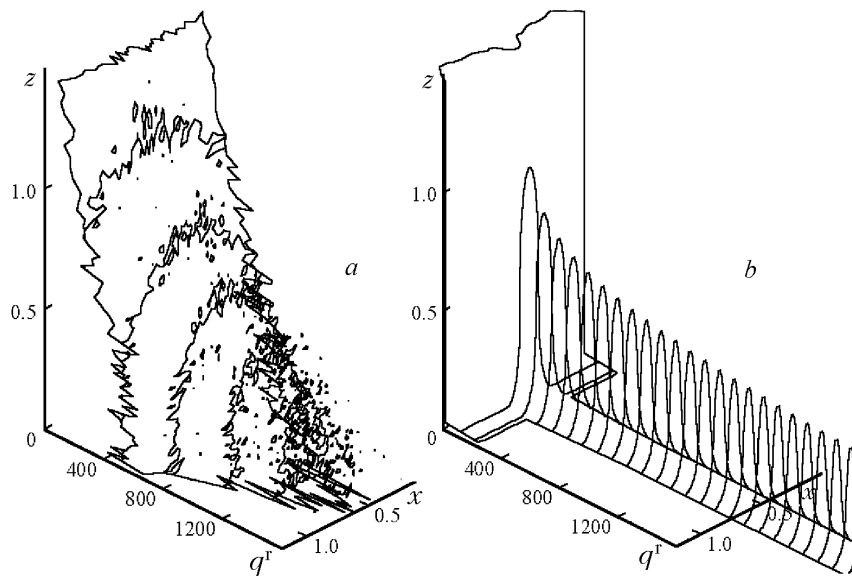


Fig. 8. Radiation flux incident on a vertical plane at a distance of 0.6 m from the flame axis: a) flow method; b) statistical method, 10^6 photons. q^r , W/m^2 ; x , z , m.

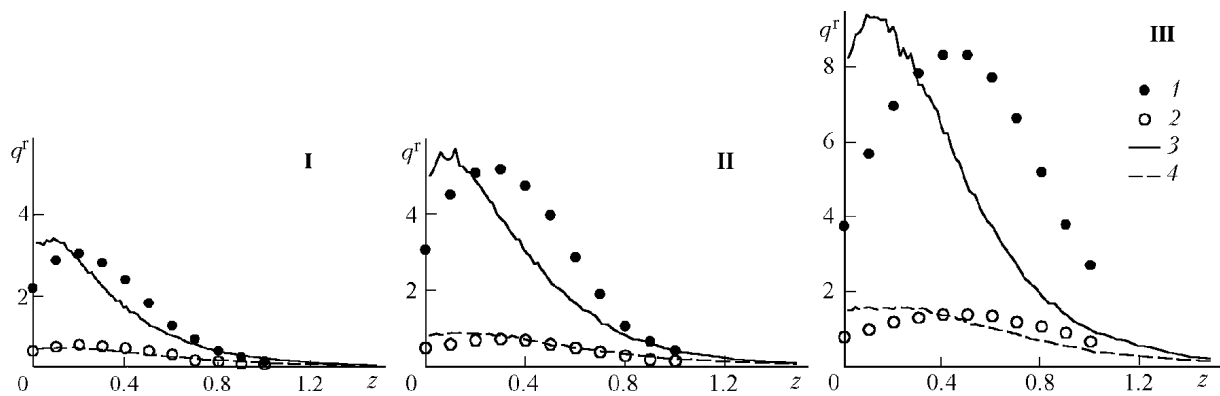


Fig. 9. Distribution of the radiation heat flux over the height. Distance from the flame axis: 1) 0.3 [10], 2) 0.58 [10], 3) 0.3, the present model, and 4) 0.58 m, the present model. I, II, and III, see Fig. 2 for the notation. q^r , W/m^2 ; z , m.

The statistical method gives a more realistic space distribution (Fig. 8b), which is in agreement with measurement results. Figure 9 gives vertical profiles of radiation heat fluxes at the same points where the measurements have been made [10] (radiation-flux sensors were located at distances of 0.3 and 0.58 m from the flame axis). Noteworthy is the good agreement between the calculated and measured values of the fluxes at the point of location of the second sensor. At the same time, an appreciable difference is observed for the first sensor, which is closer to the flame axis: the calculated heat flux reaches its maximum at a smaller height than the experimental flux. A possible reason for the discrepancy is the earlier-mentioned underestimated width of the temperature profile in the zone of temperature maximum. Moreover, the experimental profiles of the temperature and the radiation flux show that a maximum flux is emitted from the flame zone which lies above the maximum of the mean temperature. This indicates a considerable effect of the turbulent temperature fluctuations on the emission of radiation (we note that their maximum (Fig. 4) lies higher than the maximum of the mean temperature). This effect was approximately allowed for in this model (see [8]); however, its further verification requires account for the effect of concentration fluctuations and the contribution of momenta of higher order in averaging the emission of radiation.

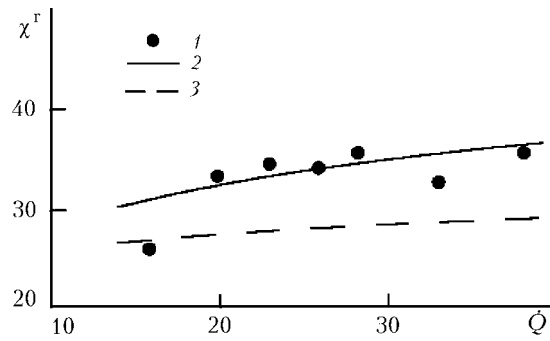


Fig. 10. Dependence of the portion of emitted energy on the heat power of the flame: 1) experiment [10]; 2) calculation by the present model with account for the influence of turbulent fluctuations on the emission of radiation [8]; 3) calculation by the present model without account for turbulent fluctuations. \dot{Q} , kW; χ^r , %.

TABLE 1. Contribution of the Time of Fulfillment of Problems to the Total Time of Processor Operation in Modeling the Flame of Power 22.9 kW on the $40 \times 40 \times 64$ Grid

Problem	Number of emitted photons, 10^5			
	1	2	4	8
Calculation of pressure and correction of velocity	0.43	0.41	0.38	0.33
Equations of motion + equations of transfer of k and ϵ	0.25	0.24	0.22	0.19
Equations of transfer of scalars + chemical reactions	0.27	0.26	0.24	0.21
Thermal-radiation transfer	0.05	0.09	0.16	0.27

We note that approximate account for turbulent fluctuations in determination of the emission of flame radiation [8] made it possible to improve the agreement of calculated and measured quantities. This is shown in Fig. 10,

where the dependence of the portion of emitted energy $\chi^r = \frac{1}{\dot{Q}} \int \frac{\partial q_j^r}{\partial x_j} dx dy dz$ (integration over the volume of the computational region) on the heat power of the flame \dot{Q} is presented.

The statistical method makes it possible to calculate the effective radiating capacity ϵ_f , which can be determined as the ratio of the number of absorbed photons to the number of those emitted. The effective optical thickness of the flame τ_f related to the effective radiating capacity is calculated from the relation $\epsilon_f = 1 - \exp(-\tau_f)$. For the three considered flames (15.8, 22.9, and 37.9 kW), the calculated value of τ_f is 0.22, 0.28, and 0.39, which approximately corresponds to optically thin flames transparent to most of the emitted radiation.

Thus, the physical model and the numerical methods used in the present work allow one to obtain an adequate description of the main parameters of turbulent diffusion flames including the concentrations of main components, velocity, temperature, and their fluctuations. Moreover, this model reproduces radiation heat fluxes emitted by the flame and incident on a remote surface.

Computational Costs. The contribution of the time of fulfillment of different subproblems to the total time of processor operation in modeling a flame of power 22.9 kW is given in Table 1. The procedure of correction of pressure and velocity which provides fulfillment of the continuity equation is the most labor-consuming. The consumption of time by the calculation of radiation transfer becomes comparable to the expenditure in performing the above procedure when the number of emitted photons exceeds 10^6 . We note that the time of calculation of radiation transfer by the statistical method depends on the number of meshes in the computational grid, on the character of space distribution of the temperature and the coefficient of absorption, and on the reflecting and emitting properties of enclosing surfaces. The calculations made in the present work showed that $4 \cdot 10^5$ emitted photons allowed an acceptable level of statistical fluctuations about the mean value of the heat flux (see Fig. 6). Thus, the computational costs of implementation of the statistical method are no higher than those of solution of other problems.

CONCLUSIONS

In modeling flames with a heat power of 15.8, 22.9, and 37.9 kW we compared the calculated data to the results of measurements of the concentrations of the main components (fuel, oxygen, carbon dioxide and monoxide), the mean temperature and velocity and their turbulent fluctuations, the profiles of the emitted heat fluxes, and the total amount of emitted energy. Despite the limitations inherent in the k - ϵ model used, we obtained good agreement with experiment.

The statistical method of calculation of radiation transfer was also compared to the flow method, which is widely used in engineering practice. The comparison showed that the latter cannot guarantee adequate calculation of the radiation heat fluxes from localized sources which are incident on remote surfaces, whereas the statistical method allows this.

In numerical calculations, we studied the dependence of the results of statistical modeling on the number of photons emitted by the radiating medium. It is shown that reliable results can be obtained under conditions of acceptable computational costs which do not exceed the costs of solution of other problems (calculation of the fields of velocity and pressure, solution of scalar equations of transfer).

NOTATION

C_p , heat capacity at constant pressure, J/(kg·K); C_μ , constant in the Kolmogorov–Prandtl formula for turbulent viscosity; D , characteristic dimension (diameter) of the burner, m; E , density of radiation energy, W/m²; Fr, Froude number; g , free-fall acceleration, m/sec²; k , kinetic energy of turbulence, m²/sec²; K_{abs} , coefficient of absorption of thermal radiation, 1/m; L_B and V_B , natural-convection scales of length and velocity, m and m/sec; L_t , space scale of turbulence, m; N , number of photons in the statistical method; q^r , radiation heat flux, W/m²; \dot{Q} , heat power of the flame, W; r , distance to the torch axis, m; T , mean temperature, K; T' , instantaneous temperature fluctuation, K; u and w , mean radial and axial velocities; u' and w' , instantaneous fluctuations of the radial and axial velocities, m/sec; V_{fuel} , linear velocity of supply of the gaseous fuel, m/sec; X_α , mole fraction of the α -component in the mixture after removal of H₂O; x_j , coordinate corresponding to the j axis, m; x , y , horizontal coordinates, m; z , vertical coordinate (equals zero at the level of the burner surface); α_k and α_L , parameters for determination of the turbulent characteristics at the burner cut; ϵ , rate of dissipation of the turbulence energy, m²/sec²; ϵ_f , effective radiating capacity of the flame; χ^r , portion of the emitted energy; θ , dimensionless temperature on the torch axis; μ_t , turbulent viscosity, Pa·sec; ω , dimensionless velocity on the torch axis; ρ , density, kg/m³; σ , Stefan–Boltzmann constant, W/(m²·K⁴); τ_f , effective optical thickness of the flame; τ_t , turbulent time scale, sec. Subscripts: abs, absorption; B, buoyancy; f, flame zone; fuel, fuel; L, length; r, radiation; surf, boundary surface element; t, turbulent; vol, internal control volume; 0, surrounding air; prime, fluctuations; max, maximum.

REFERENCES

1. J. B. Moss, in: G. Cox (ed.), *Combustion Fundamentals of Fire*, London (1995), pp. 221–272.
2. N. L. Crauford, S. K. Liew, and J. B. Moss, *Combust. Flame*, **61**, 63–77 (1985).
3. M. O. Annarumma, J. M. Most, and P. Joulain, *Combust. Flame*, **85**, 403–415 (1991).
4. K. C. Adiga, D. E. Ramaker, P. A. Tatem, and F. W. Williams, *Fire Safety J.*, **14**, 241–250 (1989).
5. K. C. Adiga, D. E. Ramaker, P. A. Tatem, and F. W. Williams, *Fire Safety J.*, **16**, 443–458 (1990).
6. Zh. Yan and G. Holmstedt, *Int. J. Heat Mass Transfer*, **42**, 1305–1315 (1999).
7. F. Liu and J. X. Wen, *Fire Safety J.*, **37**, 125–150 (2002).
8. A. Yu. Snegirev, *Inzh.-Fiz. Zh.*, **76**, No. 2, 48–56 (2003).
9. E. Gengembre, P. Cambray, D. Karmed, and J. C. Bellet, *Combust. Sci. Technol.*, **41**, 55–67 (1984).
10. J. M. Souil, P. Joulain, and E. Gengembre, *Combust. Sci. Technol.*, **41**, 69–81 (1984).
11. E. E. Zukoski, in: G. Cox (ed.), *Combustion Fundamentals of Fire*, London (1995), pp. 101–219.
12. Ç. Hirsch, *Numerical Computation of Internal and External Flows*, Chichester (1988).
13. E. P. Volkov, L. I. Zaichik, and V. A. Pershukov, *Modeling of Combustion of Solid Fuels* [in Russian], Moscow (1994).